Unstrained Element Length-Based Methods for Determining One Optimized Initial State of Cable-Stayed Bridges

Myung-Rag Jung[1], Dong-ju Min[2], Mario M. Attard[3], Moon-Young Kim[4]

[1]Graduate Student, Dept. of Civil and Environmental Engineering, Sungkyunkwan University,
[2]Graduate Student, Dept. of Civil and Environmental Engineering, Sungkyunkwan University,
[3]Associate Professor, School of Civil and Environmental Engineering,
The University of New South Wales, Sydney, NSW 2052, Australia,
[4]Professor, Dept. of Civil and Environmental Engineering, Sungkyunkwan University, 2066, Seobu-Ro, Jangan-gu, Suwon-si, 440-746, S. Korea(corresponding author)

Abstract— *Two robust procedures evaluating all unstrained element lengths are presented to find one practically optimized initial shape of cable-stayed bridges under dead loads. An analytical method based on the continuous girder model accounting for P-Δeffects due to stay-cable tensions is first proposed to calculate optimized cable tensions and unstrained element lengths without recourse to refined nonlinear FE analysis method. And then it is addressed how the G.TCUD method [10] developed for suspension bridges should be applied to determine an optimized initial state of cable-stayed bridges. For this, the extended nonlinear formulations of the co-rotational frame element as well as the elastic catenary cable element are briefly summarized by adding unstrained lengths of all finite elements to the unknown. Finally, based on the unstrained lengths determined from two methods, the unstrained length methods are presented to effectively perform nonlinear FE analysis of cable stayed bridges subjected to various load combinations. Consequently accuracy and effectiveness of the proposed schemes are demonstrated by showing that not only the unstrained lengths of a long-span cable-stayed bridge model by the analytical method are nearly same as those by the G.TCUD method but also these two methods lead to essentially one optimized initial configuration which is in suit with the target geometry.*

Keywords— Initial shaping, G.TCUD, elastic catenary cable element, co-rotational frame element, unstrained length, cable-stayed bridge

I. INTRODUCTION

Generally one initial configuration satisfying the equilibrium condition between external dead loads and internal member forces including cable tensions should be predetermined in the preliminary design stage of cable-supported bridges because cable members cannot be defined in the stress-free state. Moreover it is of extreme importance to obtain the minimized bending moment distributions by determining optimized cable tensioning forces because the internal forces due to dead loads can be significantly large as the span length of cable bridges is increased. This analysis process finding one initial equilibrium state close to the target configuration of cable structures under full dead loads is referred to as shape finding, form finding or initial shape analysis.

With relation to shape finding problems of cable-stayed bridges, a set of optimized tensioning forces for stay-cables should be found such that the vertical displacements of the main girder vanish except for the fabrication camber and the horizontal displacements of the pylon are minimized within the allowable limit. Otherwise, huge bending moments in the deck and pylons of cable-stayed bridges under dead loads can be induced due to the P - Δ effect by horizontal or vertical components of the cable tension. Furthermore, in case of fan- and harp-typed cable-stayed bridges, one *practically* optimized initial state should be searched because there can exist several initial configurations. Particularly as the span length of cable-supported bridges is greatly increased, the maximum bending moment occurring in the main girder and the pylon can become rapidly outsized depending on the fabrication camber and the balanced condition with respect to self-weights.

Until now, to find the initial state solution of cable-stayed bridges, various analysis methods have been developed such as the zero displacement method [1], the force equilibrium method [2], the optimization method [3, 4, 5], the initial force method [6], the TCUD (Target Configuration Under Dead loads) method [7], and the combination method of initial force method and TCUD method [8, 9]. However, it is judged that the optimized cable tensioning problem of cable-stayed bridges is still

challenging because the slight variation of cable tension forces can result in massive bending moments in the main girder or pylons.

Particularly it is worth mentioning the unstrained element length-based method [10] generalizing TCUD method recently proposed for finding *an optimized initial shape of suspension bridges under dead load*. In that study, the extended tangential stiffness matrices of the frame element as well as the cable element were derived by adding unstrained lengths of all finite elements to the unknown. And the unstrained element length-based methods including the G.TCUD method were then proposed based on Newton iteration method. Eventually it was demonstrated through numerical application that one *ideally* optimized initial configuration for typical suspension bridges subjected to full dead loads can be successfully found such that not only the converged state well conformed to the designed configuration but also bending moments in the main girder were minimized and moments in the tower were negligibly small. For cable-stayed bridges contrary to suspension bridges, it is questionable whether the nonlinear analysis methods proposed for suspension bridges can be straightforwardly applied to long-span cable-stayed bridges or not.

On the other hand, some analytical method has been proposed to get the trial initial state solution of cable bridges. The study by Chen *et. al* [2], which is based on the continuous beam model virtually supported at the points anchored by stay cables and a constraint condition of horizontal displacements at the top of the pylon, is worth referring in case of cable-stayed bridges. However, most of initial state solutions obtained analytically by these methods might not provide one optimized initial configuration due to the combined action of fabrication cambers and horizontal tension components of cable members in case of self-anchored cable-stayed bridges. In other words, for cable-stayed bridges having fabrication cambers, bending moments and reaction forces of the continuous stiffening girder supported virtually at the points anchoring by cable elements can be inaccurately evaluated due to horizontal tensions because it is subjected to horizontal tension components of cable members as well as self-weights. Furthermore, stay-cables in case of long-span cable-stayed bridges are so long that it can be sometimes required to improve the accuracy in calculating their unstrained lengths.

This paper intends to propose two robust procedures evaluating all unstrained element lengths to find one practically optimized initial shape of cable-stayed bridges under dead loads:

1. *An improved analytical method* based on the continuous girder model accounting for $P-\Delta$ effects of the main girder due to cable tensions is first proposed to calculate optimized cable tensions and unstrained element lengths without recourse to refined nonlinear FE method.

2. And then it is addressed how *the G.TCUD method* [10] developed for suspension bridges should be applied to determine an optimized initial state of cable-stayed bridges.

3. For this, the extended nonlinear formulations of the frame element as well as the cable element are briefly summarized by adding unstrained lengths of all finite elements to the unknown.

4. Finally, based on the unstrained lengths determined from two methods, *the unstrained length methods* are presented to effectively perform nonlinear FE analysis of cable-stayed bridges subjected to various load combinations.

5. For a long-span cable-stayed bridge example having two intermediate piers, accuracy and effectiveness of the proposed two schemes are demonstrated by showing that not only the unstrained lengths by the analytical method are nearly same as those by the G.TCUD method but also these two methods lead to essentially one optimized initial configuration which is in suit with the target geometry.

6. In particular, amplified effects of the fabrication camber and the weight balancing between center and side spans on the initial state solution are carefully investigated through the bridge example.

II. NONLINEAR ELASTIC CATENARY CABLE AND FRAME ELEMENTS

Jayaraman and Knudson [11] have firstly proposed an elastic catenary cable element from the exact solution (Irvine [12]) of the elastic catenary cable equation under its self-weight. And a frame element for geometrically nonlinear analysis of plane frames has been developed by several researchers (Pacosteand Eriksson [13], Crisfield [14], Leand Battini [15]). In this section, the unstrained length-based frame and cable element presented in Jung *el al*. [10] are briefly formulated to develop the G.TCUD method and the corresponding unstrained length method in the subsequent sections.

Consider an elastic catenary cable element suspended between two points $i(0,0)$ and $j(L_x, L_y)$ as shown in Fig. 1. By integrating equilibrium equations exactly, the following compatibility condition can be derived as a function of the nodal forces F_1 and F_2 at the node *i* and the unstrained length L_o as

$$L_x = -\frac{F_1 L_o}{EA_o} + \frac{F_1}{w}\left\{\sinh^{-1}\left(\frac{F_2 - wL_o}{F_1}\right) - \sinh^{-1}\left(\frac{F_2}{F_1}\right)\right\} \tag{1a}$$

$$L_y = -\frac{F_2 L_o}{EA_o} + \frac{wL_o^2}{2EA_o} + \frac{1}{w}\left(T_q - T_p\right) \tag{1b}$$

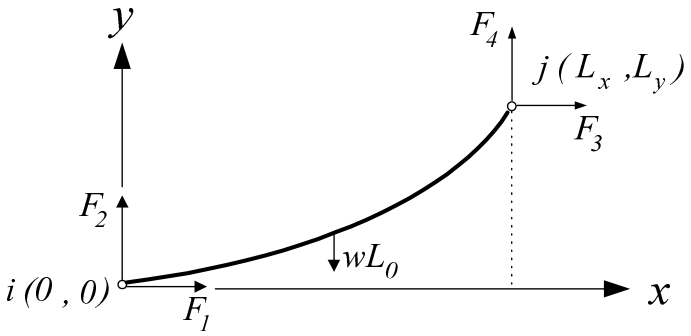

FIGURE 1 AN ELASTIC CATENARY CABLE ELEMENT SUBJECTED TO ITS SELF-WEIGHT AND NODAL FORCES

where $T_p = \sqrt{F_1^2 + F_2^2}$; $T_q = \sqrt{F_1^2 + \left(wL_o - F_2\right)^2}$; EA_o = the axial rigidity; w = self-weight per unit length.

Now partial differentiation of both sides of Eq. (1) yields the following incremental relationships:

$$\begin{Bmatrix}\Delta L_x \\ \Delta L_y\end{Bmatrix} = \begin{bmatrix}\partial L_x/\partial F_1 & \partial L_x/\partial F_2 \\ \partial L_y/\partial F_1 & \partial L_y/\partial F_2\end{bmatrix}\begin{Bmatrix}\Delta F_1 \\ \Delta F_2\end{Bmatrix} + \begin{bmatrix}\partial L_x/\partial L_o \\ \partial L_y/\partial L_o\end{bmatrix}\Delta L_0 \tag{2a}$$

$$\Delta L_x = \Delta U_3 - \Delta U_1 \text{ and } \Delta L_y = \Delta U_4 - \Delta U_2 \tag{2b, c}$$

Consequently the inverse of the flexibility matrix in Eq. (2a) leads to incremental equilibrium equations of an elastic catenary cable element as follows;

$$\Delta \mathbf{F_c} = \mathbf{K_c}\,\Delta \mathbf{U_c} + \mathbf{K_{cu}}\,\Delta L_o \tag{3}$$

Where $\Delta\mathbf{F_c}$ = the incremental nodal force vector; $\mathbf{K_c}$ = the tangential stiffness matrix; $\Delta\mathbf{U_c}$ = the incremental displacement vector; $\mathbf{K_{cu}}$ = the stiffness matrix related to the unstrained length. It should be emphasized that all the stiffness terms in Eq. (3) are fully used for calculating the extended tangential stiffness matrix in case of the TCUD methods but the last term in Eq. (3) vanishes in the unstrained length method because the unstrained cable length L_o is kept constant. In addition to this, one of nodal forces F_1 and F_2 of long stay-cable members is assumed to remain unchanged in developing an analytical method in section 3.2. Consequently it is worth pointing out that Eq. (1) should be iteratively solved with keeping one of F_1, F_2 and L_o a fixed value in order to resolve the state determination problem of elastic catenary cable elements.

On the other hand, Fig. 2 shows nodal displacements and deformation components of a frame element with respect to the co-rotational coordinate system at the initial and the deformed state where the nodal displacement and force vector may be defined as follows;

$$\mathbf{U_f}^T = \left(U_1, U_2, U_3, U_4, U_5, U_6\right) \tag{4a}$$

$$\mathbf{F_f}^T = \left(F_1, F_2, F_3, F_4, F_5, F_6\right) \tag{4b}$$

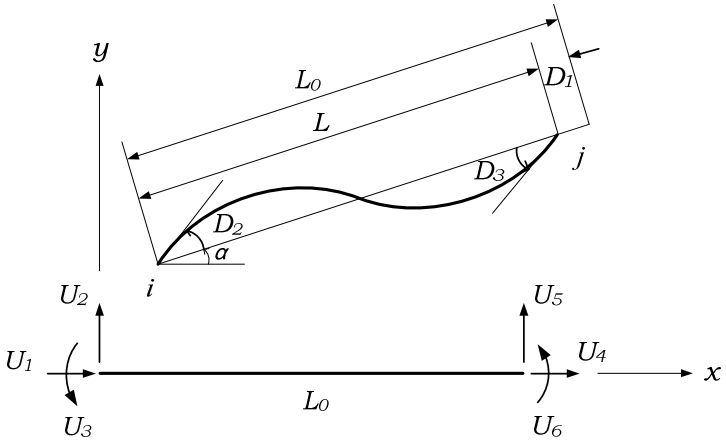

FIGURE 2 NODAL DISPLACEMENTS AND PURE DEFORMATIONS OF A NONLINEAR FRAME ELEMENT

Large rigid-body motions but the small deformations are assumed in this formulation. Removing rigid body modes from nodal displacement, the three pure deformations consisting of the axial deformation and relative rotations can be determined as follows;

$$\mathbf{D} = \begin{bmatrix} D_1 \\ D_2 \\ D_3 \end{bmatrix} = \begin{bmatrix} L - L_o \\ U_3 - \alpha \\ U_6 - \alpha \end{bmatrix} \tag{5}$$

where L = the chord length between two element nodes. Note that L_o is the element length computed as the distance between the nodal points in the TCUD method but the unstrained element length which should be updated iteratively in the G.TCUD method [10].

Then the chord length L and rigid body rotation α are calculated as

$$L = \sqrt{\left(x_j - x_i + U_4 - U_1\right)^2 + \left(y_j - y_i + U_5 - U_2\right)^2}$$

$$\tan\alpha = \frac{y_j - y_i + U_5 - U_2}{x_j - x_i + U_4 - U_1}$$

where $(x_i, y_i), (x_j, y_j)$ = the nodal coordinates in the global coordinate system.

Now force-deformation relationships of the beam-column element considering the bowing effect and $P-\delta$ effect can be expressed as follows;

$$P_1 = EA\left(\frac{D_1}{L_o} + \frac{2D_2^2 - D_2 D_3 + 2D_3^2}{30}\right) \tag{6a}$$

$$P_2 = \left(\frac{4EI}{L_o} + \frac{2P_1 L_o}{15}\right) D_2 + \left(\frac{2EI}{L_o} - \frac{P_1 L_o}{30}\right) D_3 \tag{6b}$$

$$P_3 = \left(\frac{2EI}{L_o} - \frac{P_1 L_o}{30} \right) D_2 + \left(\frac{4EI}{L_o} + \frac{2P_1 L_o}{15} \right) D_3 \tag{6c}$$

Referring to [10], the incremental equilibrium equation of aframe element cans beobtainedin the global coordinate system as follows;

$$\Delta \mathbf{F_f} = \mathbf{K_f}\ \Delta \mathbf{U_f} + \mathbf{K_{fu}} \Delta L_o \tag{7}$$

Where $\mathbf{K_f}$, $\mathbf{K_{fu}}$ = the tangential stiffness and the unstrained length-related stiffness matrix, respectively, which can be expressed as

$$\begin{aligned} \mathbf{K_f} &= \mathbf{R}^{\mathbf{T}} (\mathbf{k}_\mathbf{e}^* + \mathbf{k}_\mathbf{d}^* + \mathbf{k}_\mathbf{g}^*) \mathbf{R} \\ \mathbf{K_{fu}} &= \mathbf{R}^{\mathbf{T}} \mathbf{k}_\mathbf{fu}^* \end{aligned} \tag{8a, b}$$

where $\mathbf{R}$ = the coordinate transformation matrix; $\mathbf{k}_\mathbf{e}^*$, $\mathbf{k}_\mathbf{d}^*$, $\mathbf{k}_\mathbf{g}^*$ and $\mathbf{k}_\mathbf{fu}^*$ = the elastic stiffness, stiffness due to member deformations, geometric stiffness due to member forces and the unstrained length-related stiffness matrices, respectively, in the co-rotational coordinate system. Their detailed forms are presented in Appendix.

III. AN ANALYTICAL METHOD FOR THE INITIAL SHAPING ANALYSIS OF CABLE-STAYED BRIDGES

To find one optimized initial configuration of cable-stayed bridges under dead loads analytically without nonlinear FE analysis, basic assumptions are given in section 3.1 and then an analytical procedure determining all the unstrained element lengths is proposed in section 3.2.

3.1 Basic assumptions for developing the analytical method

First of all, it is assumed that in order to localize bending moments in the main girder due to dead loads, the stiffening girder is virtually supported at the nodal points anchored by stay cables so that vertical displacements should not occur at those points except for the fabrication camber. This assumption usually leads to the minimized bending moment distribution of the stiffening girder.

Second, the self-weights of a center span and two side spans in case of self-anchored cable-stayed bridges should be well balanced which can result in minimization of bending moments in pylons.

Third, it is assumed that the stay-cable element having relatively small cable lengths is *parabolic* under self-weights and nodal forces can be decomposed into the pre-tension T_θ and the vertical reaction component $wL_o/2$ as shown in Fig. 3. Also, the unstrained length L_o of the inclined stay cables can be evaluated by solving the cubic equation of Eq. (9) when their nominal tension T_θ and the chord length l are given:

$$T_\theta^3 + \frac{EA_o}{L_o}(L_o - l)T_\theta^2 - \frac{EA_o(wL_o\cos\alpha)^2}{24} = 0 \tag{9}$$

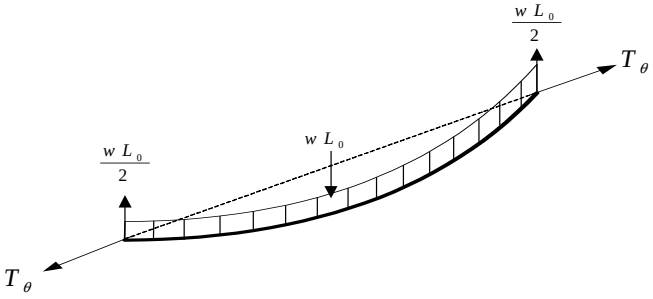

FIGURE 3 FREE BODY DIAGRAM OF A PARABOLIC CABLE ELEMENT UNDER ITS SELF-WEIGHT

Fourth, in case of extremely long-span cable-stayed bridges, the length of stay cables near the back-stay cable is so long that some deviation from the accurate solution can occur if only one parabolic cable element is used for each stay cable member. In this case, one stay cable member needs to be regarded as an elastic catenary cable element instead of a parabolic cable element.

Fifth, the chord length l in Eq. (9) in applying the analytical method is evaluated using the initial distance between two anchor points of each stay cable because main girder and the pylon subjected to dead loads and optimized cable tensions are well balanced enough to experience negligibly small displacements.

3.2 An analytical method for determining an optimized initial state of cable-stayed bridges

In case of cable-stayed bridges, nominal tensions and unstrained lengths of stay cables are usually determined from reaction forces R_i obtained through linear elastic analysis of the continuous girder model virtually supported at anchored points under only dead loads (see Fig. 4(a)). However, if geometrically nonlinear analysis for the full bridge model is performed based on them, globally huge bending moments due to P-Δ effect by horizontal tension components of stay cables can be inevitably induced in the main girder having the fabrication camber.

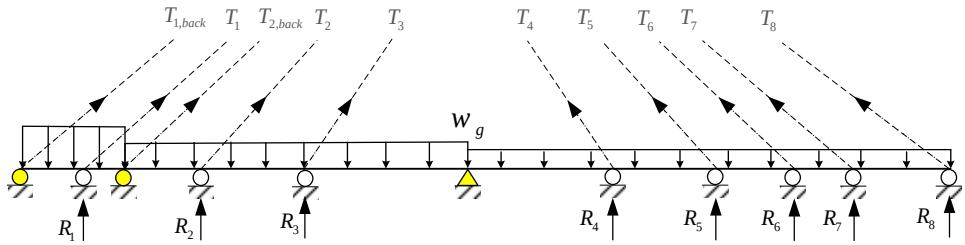

FIG 4 (A) A MAIN GIRDER SUBJECTED TO ITS SELF-WEIGHT ONLY

To get the optimized initial state solution, tension components of stay cables are suitably modified so that those bending moment in the girder should be completely excluded except for local moments. This problem can be overcome by analyzing the continuous beam subjected to its self-weight and updated tension components of stay cables simultaneously through some iteration process. In other words, the continuous girder model subjected to not only dead loads but also horizontal cable tensions as shown in Fig. 4(b) is newly considered to get rid of those global moments and to generate only local moments in the initial configuration of the main girder. In that case, modified reaction forces R_i' and corresponding cable tensions can be evaluated from linear elastic analysis of the improved girder model. And it is necessary to update horizontal cable tensions through some iteration loop because those nominal tensions of stay cables are not known in advance.

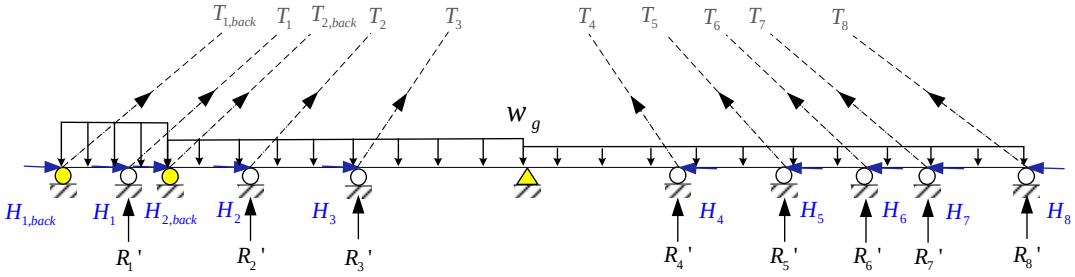

FIG 4 (B) A MAIN GIRDER SUBJECTED TO BOTH ITS SELF-WEIGHT AND THE HORIZONTAL TENSIONS OF STAY CABLES

FIGURE 4 HALF MODELS OF THE CONTINUOUS MAIN GIRDER WITH FABRICATION CAMBERS IN A CABLE-STAYED BRIDGE

Now for cable-stayed bridges with fabrication cambers subjected to dead loads, an analytical calculation procedure to make internal moment distributions minimized and to provide the corresponding unstrained lengths of all elements is given including the iteration loop of cable tensions as follows;

Step 1) Build a structural model for the continuous stiffening girdersupported vertically at the points anchoring by stay-cables as shown in Fig. 4.

Step 2) after the iteration index *k* is set to be zero, calculate the initial reaction forces $R_i^{(o)}$ at the anchor points of the continuous main girder subjected to not only its self-weight but also the initial horizontal tension component $H_i^{(o)}$ of stay cables which are zero in the first iteration process but are newly updated in the subsequent iterations.

Step 3) Enter the iteration process: $k = k + 1$

Step 4) Calculate the updated reaction force $R_i^{(k)}$ at the anchor pointsof the continuous main girder subjected to not only its self-weight but also the horizontal tension $H_i^{(k-1)}$.

Step 5) Evaluate the updated horizontal tension $H_i^{(k)}$ of the *i-th* stay cable using one of the following two cases:

I) In case of relatively short stay cables (see assumption 3), determine the nominal tension $T_{s,i}^{(k)}$ of the stay cable and the axial forces $P_{i,g}^{(k)}$, $P_{i,p}^{(k)}$ of the main girder and the pylon, respectively, by invokingthe following equilibrium conditionat two anchorage pointsof the stay cable (see Fig. 5):

$$\begin{aligned} T_{s,i}^{(k)} \sin\theta_i &= R_i^{(k)} + W_{s,i}/2 \\ T_{s,i}^{(k)} \cos\theta_i &= H_i^{(k)} \\ H_i^{(k)} &= P_{g,i+1}^{(k)} - P_{g,i}^{(k)} \\ T_{s,i}^{(k)} \sin\theta_i &= P_{p,i+1}^{(k)} - P_{p,i}^{(k)} - W_{s,i}/2 \end{aligned} \tag{10}$$

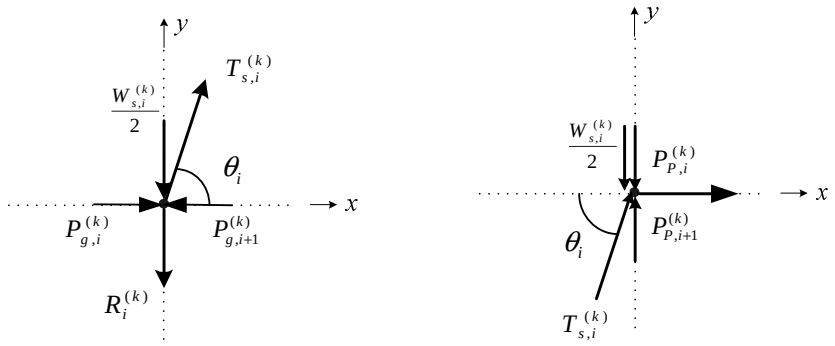

FIGURE 5 FREE BODY DIAGRAMS AT TWO ANCHORAGE POINTS OF ONE STAY CABLE

where θ_i = the inclination angle; $W_{s,i}$ = the self-weight of the *i-th*stay cable.

II) In case of relatively long stay cables (see assumption 4), solve the compatibility equation (1) of an elastic catenary cable element derived as a function of the nodal forces and the unstrained length where note that $F_2\ (=R_i^{(k)})$ is a known value calculated in Step 4) (refer to Fig. 6). Accordingly Newton iteration process is executed using the incremental equation (11) to find two unknowns L_o, $F_1(=-H_i^{(k)})$ where their initial values are chosen from Eq. (9) and (10).

$$\Delta L_x = \frac{\partial L_x}{\partial F_1}\Delta F_1 + \frac{\partial L_x}{\partial L_o}\Delta L_o \quad , \quad \Delta L_y = \frac{\partial L_y}{\partial F_1}\Delta F_1 + \frac{\partial L_y}{\partial L_o}\Delta L_o \tag{11}$$

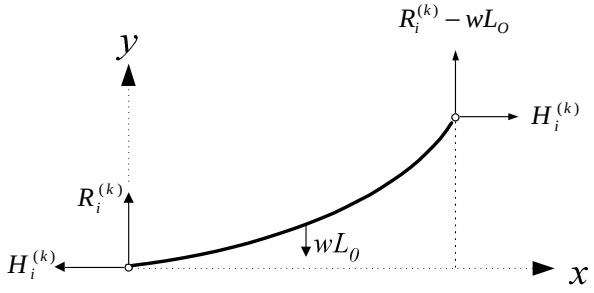

FIGURE6A STAY CABLE TREATED AS AN ELASTIC CATENARY CABLE IN THE K-TH ITERATION PROCESS

Step 6) Evaluate the horizontal tension $H_{back}^{(k)}$ of the back-stay cable: its nominal tensions cannot be evaluated from Eq. (10) due to existence of real vertical supports. Moreover it is well known that back-stay cable tensions cannot be uniquely determined in case of fan- or harp-typed cable-stayed bridges. Practically this can be calculated by analyzing the pylon model with the roller support at the node anchored by back-stay cables and subjected to horizontal tension components of stay-cables evaluated in Step 5) as shown in Fig. 7.

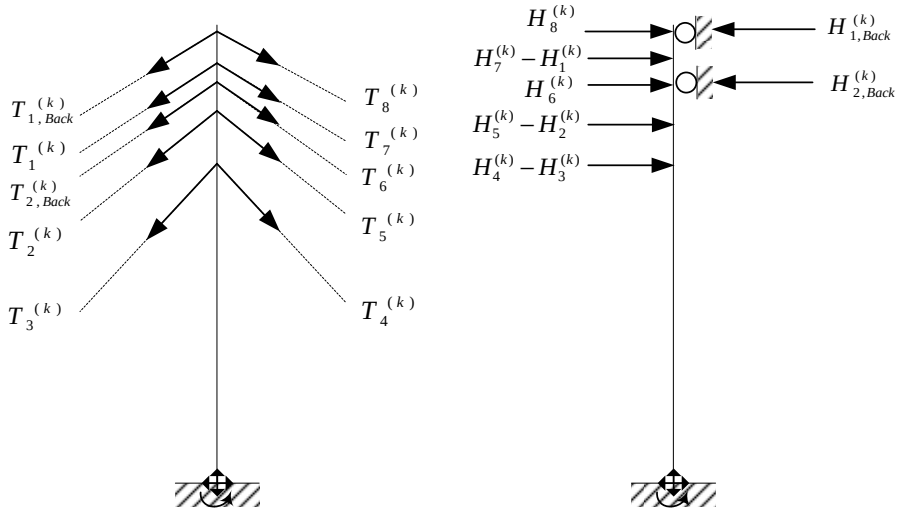

(A) A PYLON SUBJECTED TO NOMINAL CABLE TENSIONS (B) FREE BODY DIAGRAM OF A PYLON UNDER HORIZONTAL TENSIONS

FIGURE 7A PYLON SUBJECTED TO NOMINAL TENSIONS BYTHE STAY CABLE

Step 7) Check whether the nominal tensions of stay cables converge or not: If it is not converged, go to Step 3) and repeat the iteration process to Step 7). If it is converged, exit to Step 8).

Step 8) Determine the converged tensions and the unstrained lengths of all stay cables using one of the following two cases:

I) In case of relatively short stay cables, the unknown values are easily calculated using Eq. (9) and (10).

II) If the back-stay cable is relatively long, the compatibility condition of the elastic catenary cable is applied similarly to II) of Step 4) namely, Eq. (1) is iteratively solved with respect to F_2 and L_o as shown in Eq. (12) because $H_{back}^{(k)}(=-F_1)$ is determined in Step 6) (see Fig. 8).

$$\Delta L_x = \frac{\partial L_x}{\partial F_2}\Delta F_2 + \frac{\partial L_x}{\partial L_o}\Delta L_o \quad , \quad \Delta L_y = \frac{\partial L_y}{\partial F_2}\Delta F_2 + \frac{\partial L_y}{\partial L_o}\Delta L_o \tag{12}$$

Step 9) Finally evaluate the axial force and the unstrained length of frame members: the axial force of all frame members can

be determined from statics and the corresponding unstrained length using Hooke's law.

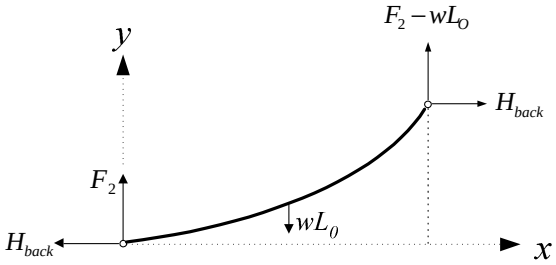

FIGURE: 8 A BACK-STAYCABLE TREATED AS AN ELASTIC CATENARY CABLE

In this study, three analytical procedures are taken into account for comparison. Fig. 9 to 11 shows flowcharts of three algorithms to determine unstrained lengths of all cable and frame elements analytically. Here the analytical method 1 (AM1) without any iteration process neglects *P*-Δ effect by horizontal tension components of stay cables which can cause huge bending moments in the main girder and the pylons due to the horizontal or the vertical components of stay cable tensions. On the other hand, both the analytical method 2 (AM2) and the analytical method 3 (AM3) can greatly reduce $P-\Delta$ effects of cable tensions owing to the updated iteration process of stay cable tensions. Here the main difference between the AM2 and AM3 is that each stay cable is modeled as an approximate parabolic cable element in the former but as an accurate elastic catenary cable in the latter. Therefore, the AM3 is expected to provide the most optimized initial state solution by treating long stay-cables as a catenary cable member.

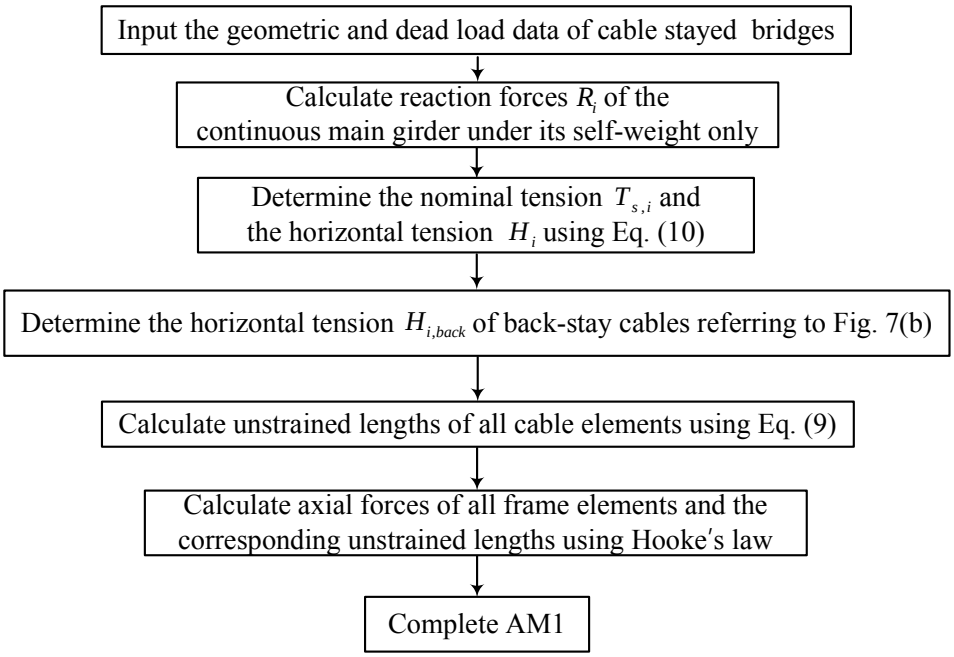

FIGURE 9 A FLOWCHART TO DETERMINE UNSTRAINED ELEMENT LENGTHS BY THE ANALYTICAL METHOD 1

IV. THE G.TCUD METHOD FOR THE INITIAL SHAPING ANALYSIS OF CABLE-STAYED BRIDGES

In this section, the generalized TCUD method is presented for initial shaping analysis of cable-stayed bridges. The TCUD and G.TCUD methods for initial shaping analysis of suspension bridges have well developed in the previous papers [7, 10]. Basically those procedures can be applied to determine the initial state of long-span cable-stayed bridges under dead loads without major modification. Accordingly in this section, the nonlinear formulation of the G.TCUD method is compactly summarized and some differences between suspension bridges and cable-stayed bridges in applying these methods are mentioned.

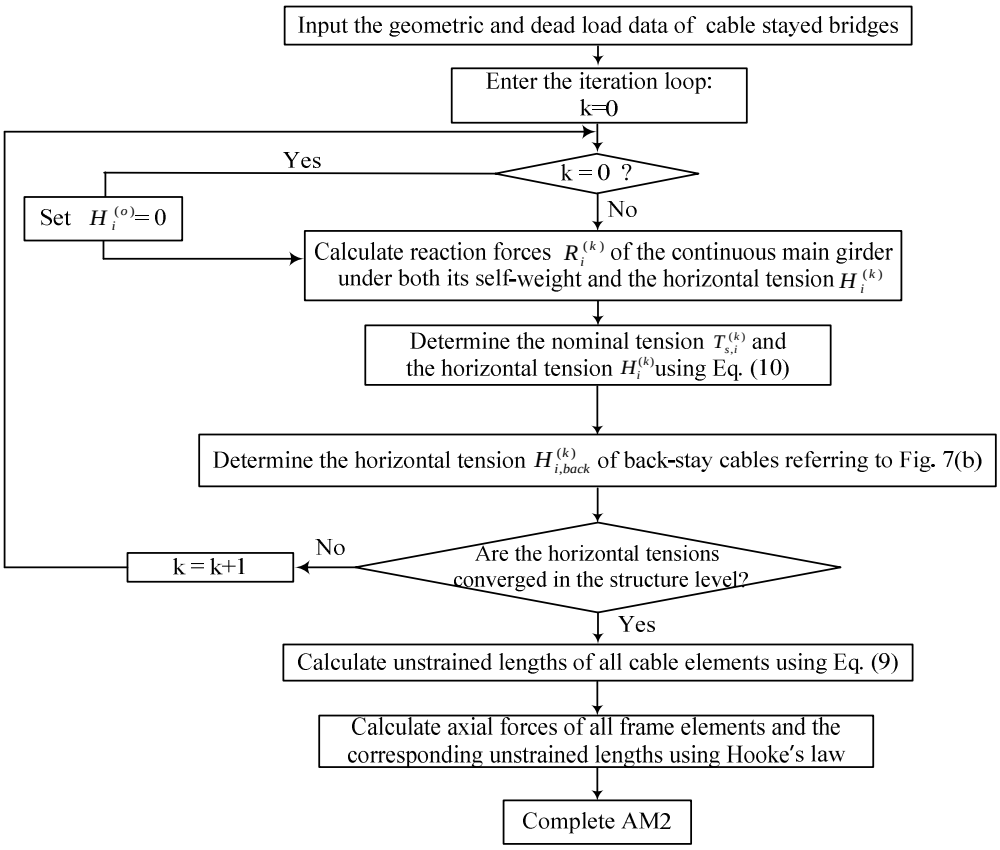

FIGURE 10 A FLOW CHART TO DETERMINE UNSTRAINED ELEMENT LENGTHS BY THE ANALYTICAL METHOD 2

The extended incremental equilibrium equation for the whole structural system accounting for unstrained element lengths as the unknown can be written as

$$\mathbf{\Delta F} = \mathbf{K_t}\,\mathbf{\Delta U} + \mathbf{K_{ul}}\,\mathbf{\Delta L_o} \tag{13}$$

where $\mathbf{\Delta F}\,(n\times 1)$ = the unbalanced load vector; $\mathbf{K_t}\,(n\times n)$ and $\mathbf{K_{ul}}\,(n\times m)$ = the tangential stiffness matrix and the unstrained length-related stiffness matrix, respectively; $\mathbf{\Delta U}\,(n\times 1)$ = the incremental nodal displacement vector; n = the number of total degree of freedom; $\mathbf{\Delta L_o}\,(m\times 1)$ = the incremental unstrained length vector where note that *m* is equal to the total number of all the cable elements in TCUD method and the number of both cable and frame elements in G.TCUD method, respectively.

Clearly additional constraint conditions should be introduced to solve the incremental equation (13) since the total number of unknown variables in Eq. (13) exceeds the total number of equations. Fig. 12 illustrates one example of the constraints applied to a cable-stayed bridge having two intermediate piers in which the arrowed degrees of freedom are additional restraints due to unstrained lengths of cable and frame elements introduced in G.TCUD method. In other words, additional geometric restraints due to cable members are the vertical displacements of the main girder at the points anchored by stay cables and the horizontal displacements of the pylon at nodal points connecting to back-stay cables. And constraints due to frame members include the axial displacements of all the nodal points in both the main girder and the pylon.

In case of suspension bridges, the horizontal displacements at the top of the tower are ideally zero and the bending moments are localized in the main girder under dead loads irrespectively of balanced or unbalanced conditions. However, it should be pointed out that all horizontal movements of the pylon cannot be perfectly

suppressed in fan- or harp-typed cable-stayed bridges. To minimize these bending moments occurring in pylons, it is of central importance for total self-weights between the center span and the side spans to be well balanced.

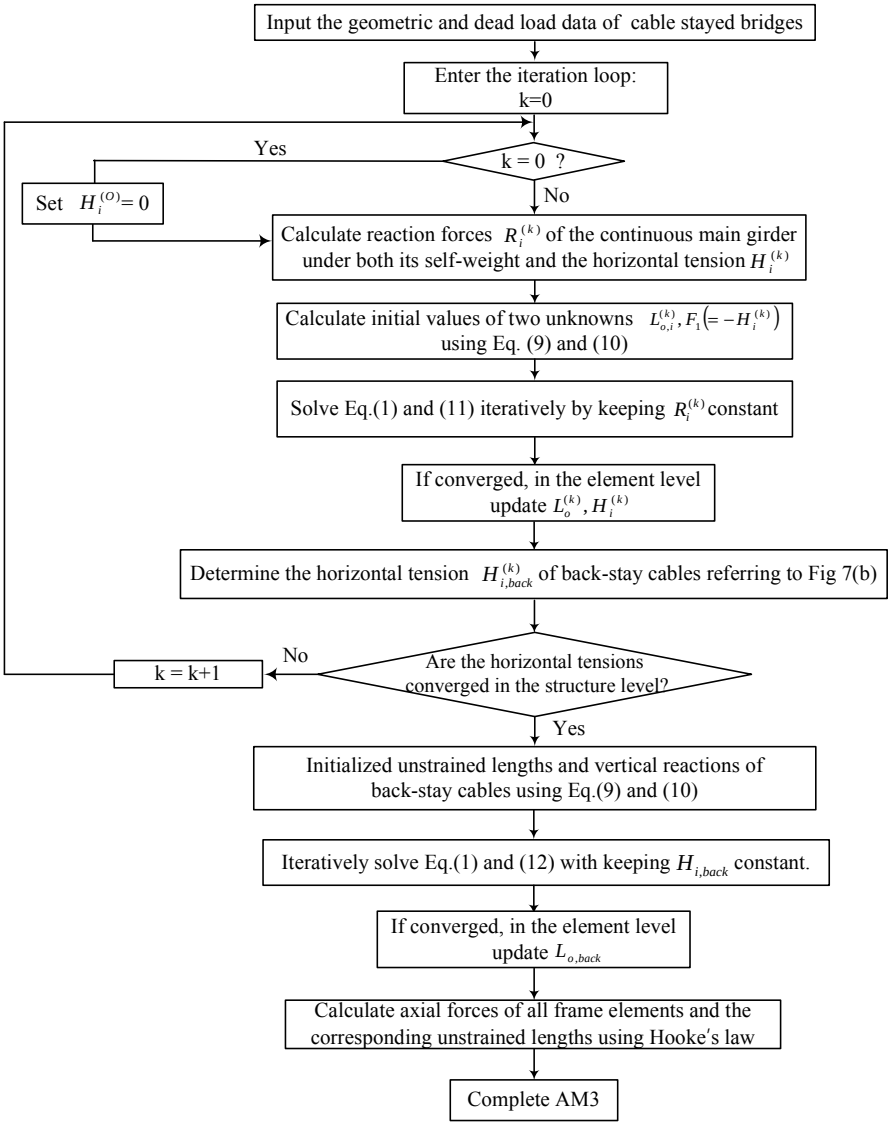

FIGURE 11 A FLOW CHART TO DETERMINE UNSTRAINED ELEMENT LENGTHS BY THE ANALYTICAL METHOD 3

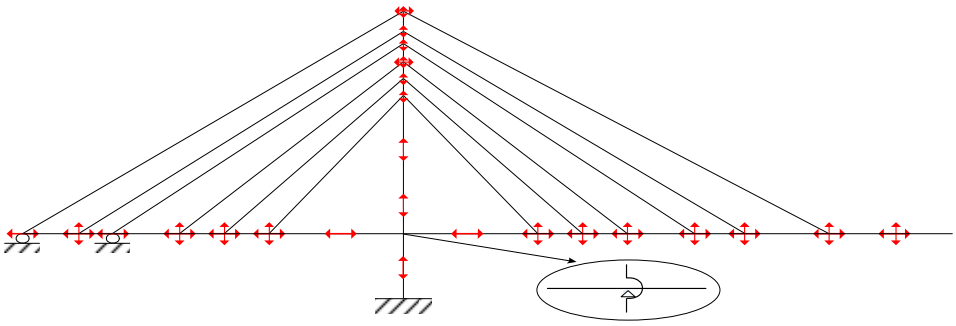

FIGURE 12 ADDITIONAL GEOMETRIC CONSTRAINTS IN THE G.TCUD METHOD FOR A HALF MODEL OF A CABLE-STAYED BRIDGE HAVING ONE INTERMEDIATE PIER

Now taking into account those additional restraints, Eq. (13) may be rewritten as

$$\mathbf{\Delta F} = \mathbf{K}_{tu}\,\mathbf{\Delta U}_u + \mathbf{K}_{ts}\,\mathbf{\Delta U}_s + \mathbf{K}_{ul}\,\mathbf{\Delta L}_o \tag{14}$$

where $\mathbf{\Delta U}_u\,((n-m)\times 1)$ = the unknown displacement vector to be determined; $\mathbf{\Delta U}_s\,(m\times 1)$ = the constrained displacement vector imposed by the designer to fulfill the target shape of the bridge; $\mathbf{K}_{tu}(n\times(n-m))$ and $\mathbf{K}_{ts}(n\times m)$ = partitioned stiffness matrices corresponding to $\mathbf{\Delta U}_u$ and $\mathbf{\Delta U}_s$, respectively.

Accordingly, the second term in the right-hand side of Eq. (14) vanishes and the other two terms result in a non-symmetric stiffness formulation as

$$(\mathbf{\Delta F}) = \begin{bmatrix}\mathbf{K}_{tu} & \mathbf{K}_{ul}\end{bmatrix}\begin{pmatrix}\mathbf{\Delta U}_u \\ \mathbf{\Delta L}_o\end{pmatrix} \tag{15}$$

Consequently the iterative G.TCUD algorithm can be represented as follows;

$$\begin{bmatrix}\mathbf{K}_{tu}^{(i-1)} & \mathbf{K}_{ul}^{(i-1)}\end{bmatrix}\begin{pmatrix}\mathbf{\Delta U}_u^{(i)} \\ \mathbf{\Delta L}_o^{(i)}\end{pmatrix} = \left(\mathbf{W} - \mathbf{F}^{(i-1)}\right) \qquad for\ \ i = 1,\ 2,\ \cdots$$

$$\begin{pmatrix}\mathbf{U}_u^{(i)} \\ \mathbf{L}_o^{(i)}\end{pmatrix} = \begin{pmatrix}\mathbf{U}_u^{(i-1)} \\ \mathbf{L}_o^{(i-1)}\end{pmatrix} + \begin{pmatrix}\mathbf{\Delta U}_u^{(i)} \\ \mathbf{\Delta L}_o^{(i)}\end{pmatrix} \tag{16}$$

where $\mathbf{W}$ = the dead load vector; $\mathbf{F}^{(i)}$ = the equivalent internal force. After the simultaneous equation (16a) having the non-symmetric stiffness matrix is solved, the total nodal displacement and the unstrained length vector are updated as seen in Eq. (16b) and the internal force vector $\mathbf{F}^{(i-1)}$ is evaluated by the state determination procedure based on the total displacements and the unstrained lengths. Particularly $\mathbf{F}^{(0)}$ denotes the internal force due to initial cable tensions and axial forces determined by the analytical procedure in section 3.1.Generally this vector vanishes in case of girder bridges but should be consistently calculated for cable bridges because it may be slowly converged or diverged if it is neglected.

***Remark 1*:** Not only the G.TCUD method provides an optimized initial state of *balanced* cable-stayed bridges but also linear analyses based on it can be conducted under various load combinations. However, similarly to analytical methods introduced in section 3, some difficulties can be caused in performing nonlinear FE analyses under extreme loads.

***Remark 2*:** Nonlinear analyses under limit load combinations including the geometry control can be easily and accurately executed through the unstrained length element method presented in the next section.

V. UNSTRAINED LENGTH METHOD FOR NONLINEAR ANALYSIS OF CABLE-STAYED BRIDGES

Basic concept of the unstrained length method (ULM) for the initial state analysis of cable-stayed bridges is similar to that for suspension bridges [10]. The unstrained length method consists of two stages. In the first stage, unstrained lengths of both cable and frame elements are pre-determined in the reasonable way and in the second stage, nonlinear FE analysis based on Newton iteration method is performed under dead loads by keeping unstrained element lengths constant. Consequently Newton-Raphson iteration algorithm for the second stage can be represented as follows;

$$\mathbf{K}_t^{(i-1)}\,\mathbf{\Delta U}^{(i)} = \mathbf{W} - \mathbf{F}^{(i-1)} \qquad for\ i = 1,\ 2,\ \cdots$$

$$\mathbf{U^{(i)}} = \mathbf{U^{(i-1)}} + \mathbf{\Delta U^{(i)}}$$
$$\mathbf{L_o^{(i)}} = \mathbf{L_o} \tag{17}$$

where $\mathbf{W}$ and $\mathbf{F^{(i)}}$ = the dead load and the internal force vector identical to those in Eq. (16). It should be again emphasized that the tangential stiffness matrix is symmetric and the unstrained lengths of all finite elements remain constant in the iteration process. In the last stage, incremental nonlinear analyses under additional live load combinations are performed by simply adding the live load $\lambda \mathbf{W_L}$ to the dead load in Eq. (17a) as follows;

$$\mathbf{K_t^{(i-1)}}\,\mathbf{\Delta U^{(i)}} = \mathbf{W} + \lambda \mathbf{W}_L - \mathbf{F^{(i-1)}} \qquad for\ i = 1,\ 2, \cdots \tag{18}$$

Particularly if some temperature increase of specific elements occurs, the unstrained length of the corresponding elements should be adjusted depending on the thermal change ΔT in which the incremental unstrained length is calculated as

$$\Delta L_o = \alpha_T \Delta T\ L_o \tag{19}$$

where α_T = the coefficient of linear thermal expansion.

With relation to the first stage of ULM, three analytical schemes determining all the unstrained lengths have been proposed in section 3.2 and G.TCUD presented in section 4. In this study, four ULMs are taken into account depending on the scheme evaluating the unstrained length as follows;

1. ULM1: the unstrained lengths of cable and frame elements obtained from the AM1 in section 3.1 are directly used in geometrically nonlinear FE analysis.

2. ULM2: the unstrained element lengths obtained from the AM2 are used.

3. ULM3: the unstrained lengths from the AM3 are used.

4. ULM4: the solution determined by G.TCUD is fully used.

Fig. 13 represents a flow chart of four ULMs. In connection with the concept of unstrained cable lengths, it is worth referring to the study by Lozano-Galant et al. [16] because it well explains what the unstrained length of cable elements means in construction stage analysis even though it is based on linear analysis.

VI. NUMERICAL EXAMPLES

In section 3 and 4, the analytical methods and G.TCUD method determining all the unstrained element lengths have been presented to find one optimized initial state of cable-stayed bridges and in section 5, four ULMs for nonlinear analysis of cable bridges subjected to additional load combinations have been proposed based on the two initial shaping analysis methods. In this section, one example determining the initial shape of self-anchored cable-stayed bridge with an intermediate pier is provided to demonstrate efficiency and effectiveness of those methods.

Incheon Bridge which connects Incheon International Airport and Songdo International city in Incheon-si is the biggest cable-stayed bridge in Korea. Figure 14 shows a structural model of Incheon bridge, and it is a long-span cable-stayed bridge with five spans of 80+260+800+260+80m, and the concrete tower is an inverse Y shape with 238.5m height. Streamlined steel box girder is suspended by 208 cables with double cable planes.

Also Figure 15 denotes the vertical camber of the main girder which is linear along the side spans and parabolic throughout the center span.

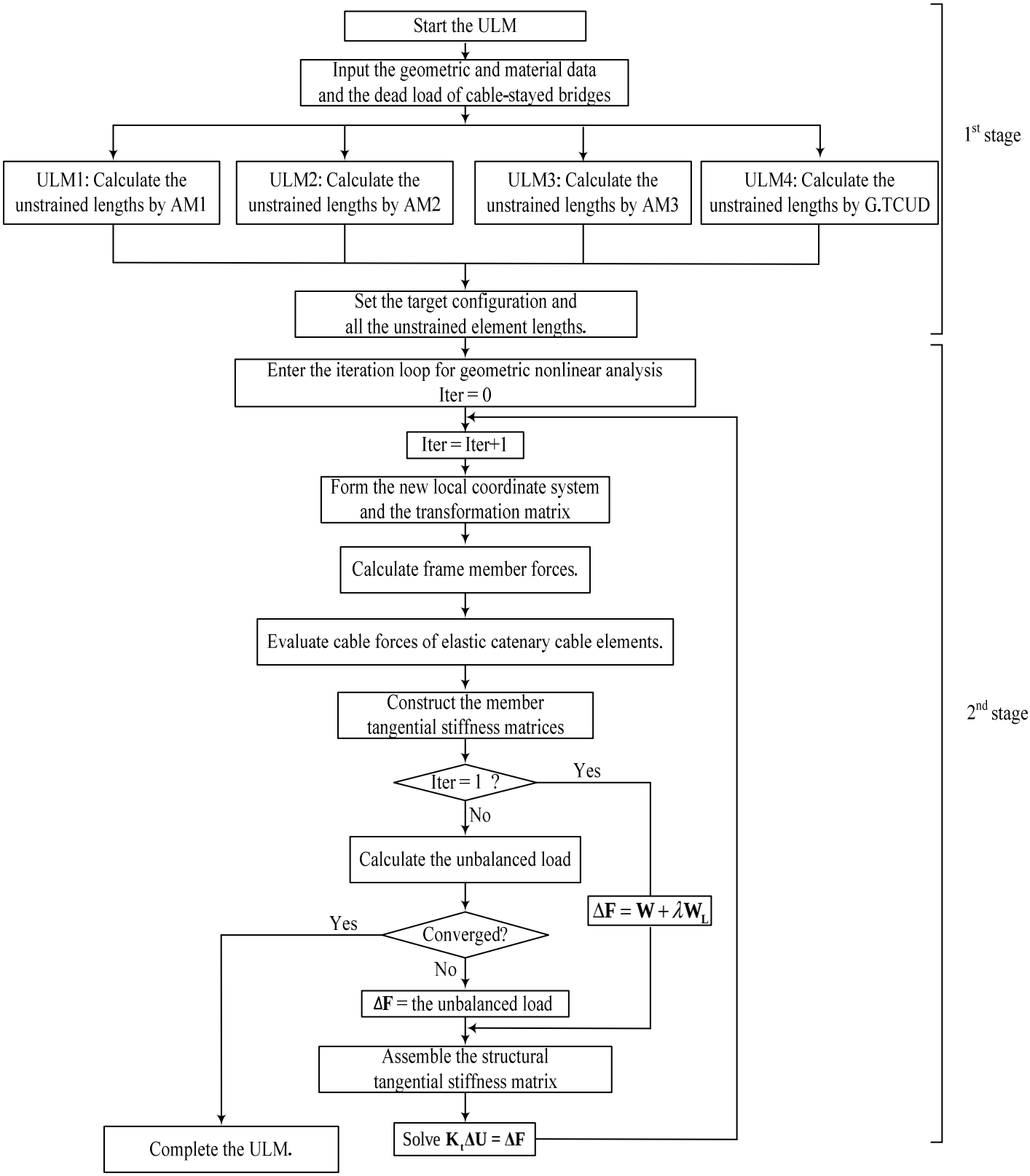

FIGURE 13 FLOW CHART OF THE UNSTRAINED LENGTH METHOD FOR CABLE-STAYED BRIDGES

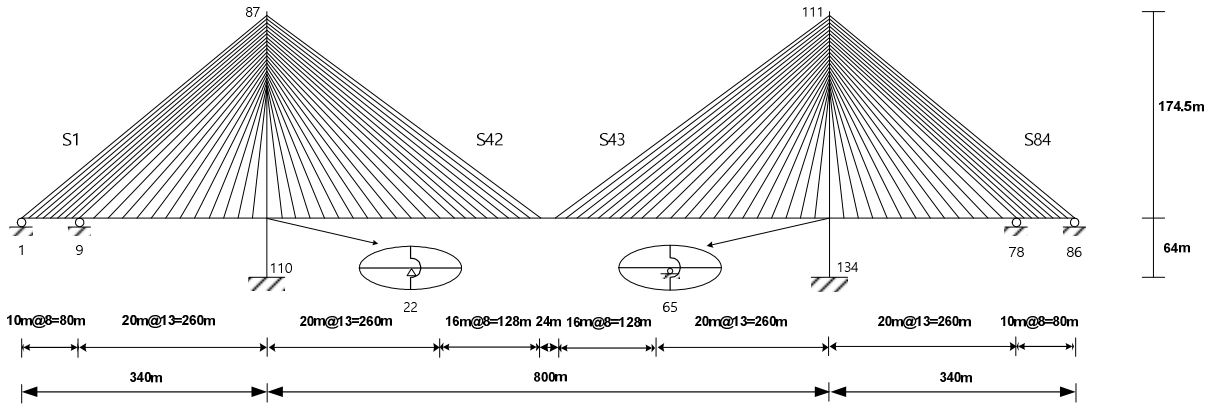

FIGURE 14 PROFILE OF INCHEON BRIDGE MODEL

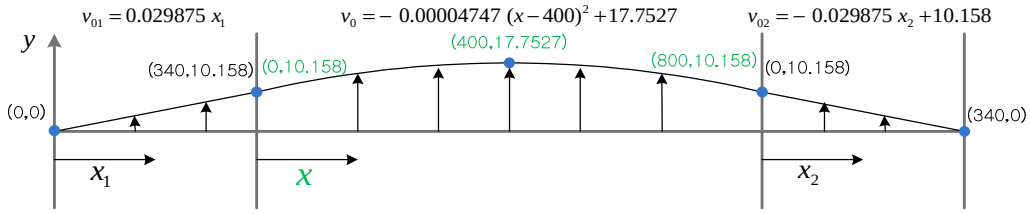

FIGURE 15 VERTICAL CAMBER OF INCHEON BRIDGE MODEL

To investigate the effects of cambers and unbalancing of self-weights, two types of the cable-stayed bridge model are basically analyzed namely, the balanced bridge having fabrication cambers and the balanced bridge with-out cambers. For comparison, the unbalanced bridge models with or without cambers are additionally explored using G.TCUD method.

Table 1 summarizes the material and cross-sectional properties of Incheon bridge model. In this model, a counter weight of 300kN/m between 6.78~36.782m and 1443.218~1473.22m along the main girder, which is neglected in case of the unbalanced bridge models, is deliberately applied to make self-weights of the center span and side spans balanced. And the supply piers are located in each side spans which means that there are four back-stay cables connected with supply piers and end piers.

TABLE1
MATERIAL AND GEOMETRIC PROPERTIES OF INCHEON BRIDGE MODEL

Structural member	E(Gpa)	A(m^2)	I(m^4)	w(kN/m)	Remarks
Girder	200	2.1203	3.1608	250.0	Counter weightof 187.5kN/m between supplemental and end piers
Tower 1	37.5	43	240.27	1065.6	0~182m
Tower 2	37.5	24.125	141.712	689.1	182m~234.5m
Cable 4	195	0.02316	-	1.86	C1~4, 8~14, 29~56, 71~77, 81~84,
Cable 6	195	0.01162	-	0.93	C5~7, 15~28, 57~70, 78~80

To get one optimized initial state solution, the following constraints are introduced in the G.TCUD method.

The essential boundary condition:

- Y-coordinates of the roller-supported points (No. 1, 9, 65 and no. 78) on the main girder
- X- and Y-coordinates of the hinged point (No. 22) on the main
- Y-coordinates of a point (No. 34) on the main girder supported by the tower
- Fixed end points (No. 110 and 134) at the base of two pylons

The additional constraints introduced in G.TCUD (displayed as arrow in Fig. 12 and as boldface in Table 2):

- Y-coordinates of points (No. 2 - 8, No. 10 - 21, No. 23 – 64, No. 66-77 and No. 79 - 85) on the main girder anchored by stay cables
- X-coordinates of points (No. 88, 96, 112 and no. 120) on the pylons anchored by back- stay cables
- X-coordinates of nodal points (No. 1 – 21, No. 23 - 86) on the main girder except for No. 22
- Y-coordinates of all nodal points on towers except for No. 110 and 134

TABLE2
UNSTRAINED CABLE ELEMENT LENGTHS IN THE CABLE-STAYED BRIDGE MODEL

Cable No.	L_O(m) by G.TCUD (1)	L_O (m) by AM1 (2)	L_O(m) by AM2 (3)	L_O(m) by AM3 (4)	ΔL_O (mm) (2)-(1)	ΔL_O (mm) (3)-(1)	ΔL_O (mm) (4)-(1)	Remarks
1	**380.523**	**380.719**	380.500	**380.515**	**195.6**	**-22.9**	**7.5**	**back stay**
3	361.298	361.359	361.247	361.296	61.3	-50.9	2.0	stay cable
5	340.801	340.781	340.790	340.800	-20.2	-11.5	0.6	stay cable
7	321.199	321.178	321.190	321.199	-21.0	-9.2	0.3	stay cable
9	**302.613**	**303.717**	302.549	**302.593**	**1103.5**	**-63.8**	**19.9**	**back stay**
11	265.955	265.976	265.935	265.955	20.9	-19.6	0.3	stay cable
13	230.850	230.866	230.836	230.850	15.6	-14.3	0.3	stay cable
15	197.363	197.357	197.361	197.363	-5.6	-2.2	-0.1	stay cable
17	167.390	167.388	167.388	167.390	-2.2	-1.5	0.2	stay cable
19	142.491	142.491	142.491	142.491	-0.1	-0.5	0.0	stay cable
21	125.750	125.751	125.749	125.750	0.9	-0.6	0.2	stay cable
23	130.386	130.409	130.385	130.386	23.2	-0.7	0.5	stay cable
25	149.821	149.855	149.819	149.820	34.0	-1.8	0.6	stay cable
27	176.397	176.446	176.395	176.397	49.3	-2.2	0.0	stay cable
29	207.714	207.767	207.700	207.713	53.2	-13.7	0.7	stay cable
31	241.495	241.567	241.476	241.494	71.9	-18.5	0.7	stay cable
33	276.984	277.075	276.961	276.983	91.4	-23.1	1.1	stay cable
35	310.296	310.415	310.249	310.294	119.1	-47.0	1.7	stay cable
37	340.455	340.589	340.405	340.453	134.0	-50.4	1.9	stay cable
39	370.992	371.142	370.935	370.991	150.3	-56.8	1.3	stay cable
41	401.914	402.093	401.835	401.912	179.4	-79.4	2.0	stay cable
42	416.900	417.040	416.862	416.899	140.4	-37.8	0.9	stay cable

Initial solutions including unstrained lengths of all cable and frame elements are firstly determined using AM1, AM2, AM3 and G.TCUD methods and then four ULMs are applied to build an initial state of the bridge model under dead loads.

Table 2 shows unstrained cable lengths and their differences evaluated by analytical methods and G.TCUD. Also, Table 3 display not only initial target coordinates including the vertical camber of the main girder but also horizontal and vertical displacements by ULMs at the nodal points of the main girder and towers connected to stay cables. Here vertical coordinates of No.1 - 86 in the second column of Table 3 denotes elevations of fabrication cambers of the main girder. Particularly nodal degrees of freedom corresponding to boldface and stared values correspond to essential boundary conditions and additional

geometric restraints introduced in G.TCUD method, respectively (also refer to Fig. 12).In addition, Fig. 16 and 17 show bending moment diagrams in the left half of the main girder and the right pylon, respectively and Fig. 18 displays fluctuations of stay cable tensions by three ULMs. Finally Table 4 shows the summary of maximum internal forces and displacements of the main girder and towers analyzed by initial shaping analysis methods for the balanced and unbalanced bridge models with the fabrication camber. On the other hand, Table 5 summarizes maximum bending moments of the main members for the balanced and unbalanced bridge without the camber. Several observations and conclusions can be drawn from the presented Tables and Figures.

TABLE 3
INITIAL COORDINATES AND NODAL DISPLACEMENTS AT THE POINT OF THE GIRDER AND TOWERS CONNECTED TO STAY CABLES BY THREE UNSTRAINED LENGTH METHODS FOR THE BALANCED BRIDGE WITH THE FABRICATION CAMBER

Node No.	Target Coord. (X,Y) (m)	ΔX by ULM1 (mm)	ΔY by ULM1 (mm)	ΔX by ULM2 (mm)	ΔY by ULM2 (mm)	ΔX by ULM3 (mm)	ΔY by ULM3 (mm)	ΔX by ULM4 (mm)	ΔY by ULM4 (mm)	Remark
1	(0.0*,**0.0**)	-9.2	0.0	0.1	0.0	0.0	0.0	0.0	0.0	roller support
5	(40*,1.195*)	-8.7	-5.2	0.0	2.0	0.0	0.0	0.0	0.0	
9	(80*,**2.390**)	-8.2	0.0	0.1	0.0	0.0	0.0	0.0	0.0	roller support
13	(160*,4.780*)	-1.1	-161.8	0.6	-18.7	0.1	-3.1	0.0	0.0	
17	(240*,7.170*)	1.1	-144.3	0.7	-22.8	0.1	-2.8	0.0	0.0	
22	(**340 , 10.158**)	0.0	0.0	0.0	0.0	0.0	0.0	0.0	0.0	Hinged support
30	(500*,15.018*)	-4.4	303.6	-1.5	51.1	-0.1	4.6	0.0	0.0	
38	(648*,17.351*)	-8.2	714.7	-3.6	181.4	-0.2	11.0	0.0	0.0	
42	(712*,17.716*)	-8.7	839.5	-3.9	221.7	-0.3	12.9	0.0	0.0	
46	(784*,17.661*)	-8.8	819.6	-3.9	215.6	-0.3	12.6	0.0	0.0	
54	(920*,16.215*)	-11.6	455.7	-5.3	95.5	-0.3	7.0	0.0	0.0	
62	(1080*,12.265*)	-15.5	112.1	-7.2	13.8	-0.5	1.7	0.0	0.0	
65	(1140*,**10.158**)	-17.6	0.0	-7.7	0.0	-0.5	0.0	0.0	0.0	roller support
69	(1220*,7.768*)	-18.6	-119.6	-8.4	-20.4	-0.6	-2.4	0.0	0.0	
73	(1300*,5.378*)	-17.7	-180.4	-8.4	-23.2	-0.6	-3.5	0.0	0.0	
78	(1400*,**2.390**)	-9.4	0.0	-7.8	0.0	-0.5	0.0	0.0	0.0	roller support
82	(1440*,1.195*)	-8.9	-4.9	-7.7	2.2	-0.5	0.0	0.0	0.0	
86	(1480*,**0.0**)	-8.4	0.0	-7.8	0.0	-0.5	0.0	0.0	0.0	roller support
88	(340 , 174*)	-202.3	1.3	-37.8	-1.4	-4.0	0.0	0.0	0.0	back-stay cable
92	(340 , 166*)	-195.8	1.3	-35.9	-1.4	-3.7	0.0	0.1	0.0	
96	(340 , 158*)	-189.3	1.3	-34.1	-1.3	-3.6	0.0	0.0	0.0	back-stay cable
104	(340 , 142*)	-174.8	1.1	-30.9	-1.2	-3.8	0.0	-0.5	0.0	
110	(**340 , -64**)	0.0	0.0	0.0	0.0	0.0	0.0	0.0	0.0	fixed support
112	(1140 , 174*)	183.9	1.3	29.5	-1.4	3.4	0.0	0.0	0.0	back-stay cable
116	(1140 , 166*)	178.3	1.3	28.1	-1.4	3.2	0.0	-0.1	0.0	
120	(1140 , 158*)	172.6	1.3	26.7	-1.3	3.1	0.0	0.0	0.0	back-stay cable
132	(1140 , 142*)	152.8	1.1	24.3	-1.2	3.3	0.0	0.7	0.0	
134	(**1140 , -64**)	0.0	0.0	0.0	0.0	0.0	0.0	0.0	0.0	fixed support

First of all, the initial state solutions by AM1 look reasonable at first glance. However, as shown in Fig. 16(b), Fig. 17(a) and the second column of Table 4 and 5, ULM1 based on unstrained lengths by AM1 gives explosively large bending moments in both the main girder and the pylon for bridge models with camber. Fundamentally this is because AM1 cannot remove magnified bending moments in the main girder with the camber and the pylons due to compressive forces transmitted by cable tensions.

Second, it is noticed in Table 3 that not only vertical displacements ΔY at nodal points on the main girder anchored by stay cables and horizontal displacements ΔX at points on the pylons anchored by back- stay cables but also axial displacements at points along the main girder and the towers by ULM4 vanish exactly which is due to constraints introduced by G.TCUD method. Particularly maximum bending moments in both the girder and the pylon by G.TCUD are ideally small in case of the balanced bridge without the camber (Table 5) while it turns out that in the balanced bridge with the camber, maximum moments in the pylon are small within the allowable limit (Table 4).

TABLE4

SUMMARY OF MAXIMUM INTERNAL FORCES AND DISPLACEMENTS FOR THE BALANCED AND THE UNBALANCED BRIDGE MODEL SHAVING THE INITIAL CAMBER

	AM1 (ULM1)	AM2 (ULM2)	AM3 (ULM3)	G.TCUD (ULM4)	G.TCUD* (ULM4*)
Max. positive moment of the main girder(kN-m)	7,852.82 (30,737.2)	7,854.31 (7,387.16)	7,858.54 (7,526.85)	7,859.57 (7,863.79)	7,859.45* (7,859.53*)
Max. negative moment of the main girder(kN-m)	-10,147.2 (-72,514.1)	-10,144.3 (-16,544.8)	-10,141.3 (-10,473.9)	-10,140.2 (-10,140.7)	-10,140.1* (-10,140.0*)
Max. compressive force of the tower (kN)	-224,694. (-215,896)	-210,324. (-214,683.)	-206,052. (-214,703.)	-214,687. (-214,687.).	-214,857.* (-214,857.*)
Max. positive moment of the right pylon (kN-m)	5,250.24 (46,232.9)	4,645.37 (4,015.2)	4,840.62 (4,986.1)	4,807.93 (4,809.22)	9,884.9* (9,885.2*)
Max. negative moment of the right pylon (kN-m)	-26,075.9 (-119,187.)	-17,021.2 (-16,998.7)	-16,681.4 (-16,176.2)	-16,818.3 (-16,816.5)	-67,119.4* (-67,119.3*)
Horizontal displacement at the top of the tower (mm)	- (202.7)	- (29.6)	- (4.0)	1.1 (1.1)	2.32* (2.31*)
Vertical displacement at the top of the tower (mm)	- (1.3)	- (-1.4)	- (0.0)	0.0 (0.0)	0.0* (0.0*)
Axial shortening of the whole main girder (mm)	- (17.6)	- (8.5)	- (0.6)	0.0 (0.0)	0.0* (0.0*)
Max. vertical displacement of the main girder (mm)	- (852.8)	- (225.2)	- (13.1)	0.6 (0.5)	0.6* (0.6*)

Consequently both G.TCUD and ULM4 clearly provide one optimized initial configuration conforming well to the target geometry in case of the balanced bridge model under dead loads as observed in Fig. 16 and 17 and Table 3. In addition, note that the absolute maximum moment of the pylon from Table 4 is 16.82 MN-m which corresponds to the small flexural stress of about 0.36 MPa (=16.818× 3/141.7) and also, the maximum bending moment of the continuous girder will decrease rapidly as the distance between anchor points of stay cables becomes small. Particularly it should be realized that both G.TCUD and ULM4 lead to completely identical initial solutions irrespective of balanced or unbalanced conditions as observed in the fourth and the fifth column of Table 4 and 5.

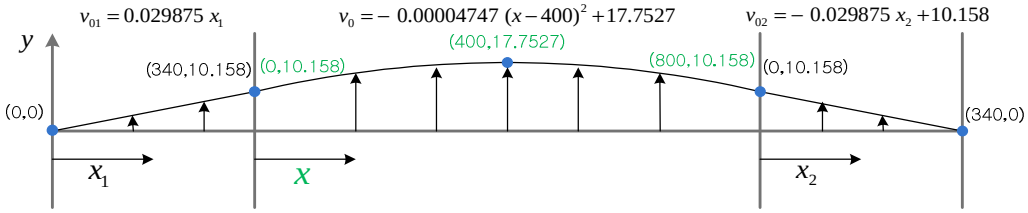

FIGURE 15 VERTICAL CAMBER OF INCHEON BRIDGE MODEL

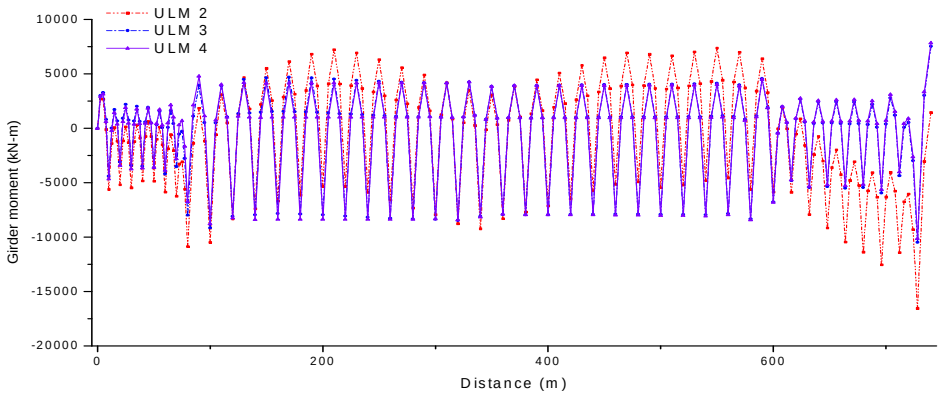

FIG 16 (A) BENDING MOMENT DIAGRAMS BY ULM2, ULM3, AND ULM4

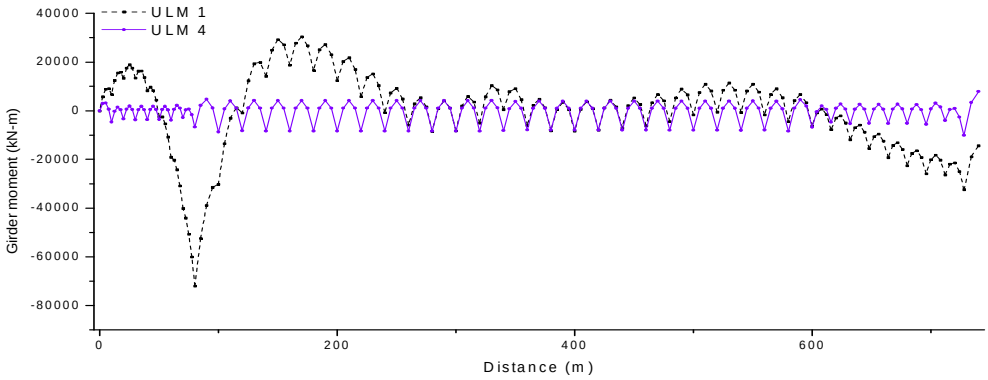

FIG 16 (B) BENDING MOMENT DIAGRAMS BY ULM1 AND ULM4

FIGURE 16 BENDING MOMENT DIAGRAMS IN THE LEFT HALFMODEL OFTHE MAIN GIRDER IN INCHEON BRIDGE (KN-M)

Third, it is noted from Table 2 to 5 and Fig. 16 and 17 that unstrained cable lengths and maximum bending moments by AM3 and ULM3 are in extremely good agreement with those by G.TCUD and ULM4 while the results by AM1and ULM1 displays large difference. Furthermore, it should be emphasized that the initial solution by AM3 shows little difference with

that by ULM3. This means that one practically optimized initial state of long-span cable-stayed bridges including unstrained element lengths can be easily determined by adopting the analytical method 3 (AM3) without recourse to relatively complicated G.TCUD.

Fourth, Table 2 to 4 and Fig. 16 and 17 reveal that overall unstrained lengths and bending moment distributions by AM2 (ULM2) show good agreement with those by the AM3 (ULM3) and the G.TCUD (ULM4) but that the initial state solutions (the fifth and sixth columns of Table 3) by ULM2 display some deviations with the target configuration. It should be pointed out that each stay-cable of Incheon bridge model is approximately modeled as a parabolic cable in AM2 which results in locally unbalanced moment distributions in pylons. Nonetheless, note that maximum bending moments by ULM2 are very small similarly to those by ULM4. Therefore, it is judged that AM2 and ULM2 can be satisfactorily applied to initial shaping analysis of cable-stayed bridges having moderate span lengths.

TABLE 5

MAXIMUM BENDING MOMENTS FOR THE BALANCED AND THE UNBALANCED BRIDGE MODELS WITHOUT THE CAMBER

	AM1 (ULM1)	AM3 (ULM3)	G.TCUD (ULM4)	G.TCUD* (ULM4*)
Max. positive moment ofthe main girder (kN-m)	7,852.82 (8,261.76)	7,853.14 (7,107.03)	7,853.12 (7,852.66)	7,853.13* (7,853.21*)
Max. negative moment of the main girder (kN-m)	-10,147.2 (-17,849.7)	-10,146.8 (-10,893.1)	-10,146.9 (-10,147.6)	-10,146.9* (-10,146.8*)
Max. positive moment of the right pylon (kN-m)	1,498.5 (1,247.1)	1,498.2 (1,189.98)	1,508.69 (1,508.61)	5,571.0* (-5,571.2*)
Max. negative moment of the right pylon (kN-m)	-1,185.6 (-17,434.5)	-1,184.4 (-3,022.32)	-1,159.01 (-1,158.71)	-53,111.7* (-53,111.6*)

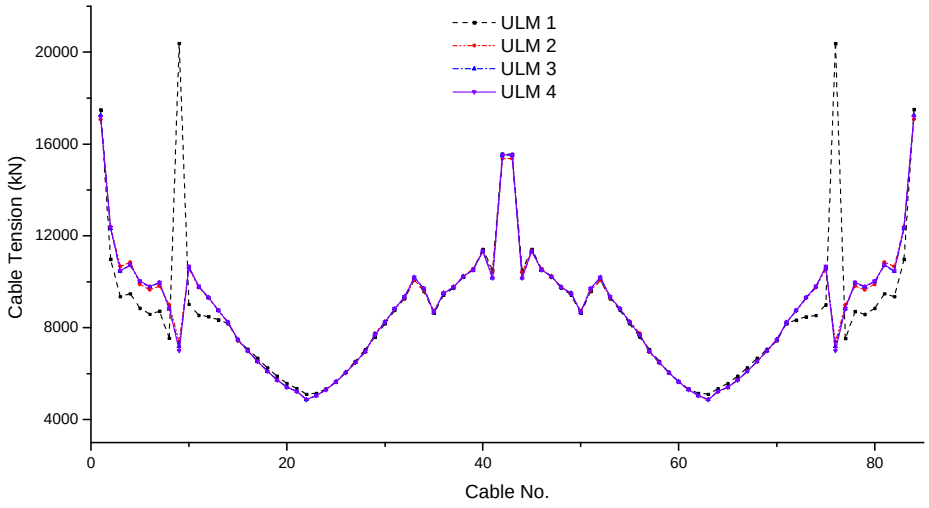

FIGURE 18 STAY CABLE TENSIONS IN THE INCHE ON BRIDGE MODEL

Finally the initial state solution of suspension bridges is usually insensitive to weight-balancing between center span and side spans because the suspension system consisting of the main cable and hangers can effectively absorbs large bending moments generated from the combined action of the fabrication camber and the horizontal compression component by the main cable even though it is a self-anchored suspension bridge.

However, initial shaping analysis of unbalanced cable-stayed bridges by G.TCUD can lead to large bending moments of pylons because cable tensions are directly transferred from the main girder to the pylons. Actually it is observed that bending moments in the main girder can be always minimized by applying G.TCUD but the maximum bending moment of the pylon for the unbalanced bridge model by G.TCUD becomes about 4 times larger than that for the balanced bridge (see the fifth and sixth columns of Table 4). This means that the weight balancing between the center span and side spans should be definitely well preserved in the preliminary design stage.

VII. SUMMARY AND CONCLUSIONS

Two unstrained-length calculation procedures for determining one optimized initial state solution of cable-stayed bridges, the analytical method and the G.TCUD method, have been presented, in which the former method is based on the continuous beam analysis and the nonlinear algebraic equations but the latter method adopts the FE Newton iteration method using the elastic catenary cable element and the consistent frame element based on the co-rotational formulation. Moreover, the unstrained length method strongly depending on the unstrained-length calculation schemes are presented to effectively perform nonlinear FE analysis of cable-stayed bridges subjected to various load combinations. Finally initial shaping analysis of a cable-stayed bridge having one intermediate pier is performed and numerical results are analyzed. The important concluding remarks can be made as follows:

1. The initial state solutions by AM1 look reasonable at first glance but ULM1 based on unstrained lengths by AM1 leads to explosively large bending moments in both the main girder and the pylon for the bridge model having the initial camber.

2. The G.TCUD introduces the corresponding additional boundary constraints instead of adding all the unstrained element lengths to the nodal unknown while the ULM adopts Newton iteration method with keeping the pre-determined unstrained lengths constant. And G.TCUD provides the optimized initial solution converging nearly to the target configuration in case of balanced cable-stayed bridges under dead loads.

3. Interestingly, even though any additional constraints in the ULM method are not enforced except for the essential boundary condition, the initial state solutions by ULM3 and ULM4 are nearly identical to those by G.TCUD irrespective of the weight-balanced condition and the fabrication camber.

4. Initial state solutions by AM3 and ULM3 are in excellently good agreement with those by G.TCUD and ULM3 while the results by AM1and ULM1 display large difference. Furthermore, the initial solution by AM3 shows little difference with that by ULM3, which means that one optimized initial state of balanced cable-stayed bridges can be easily found by adopting AM3 without recourse to relatively complicated G.TCUD.

5. Practically AM2 and ULM2 can be applied to the initial shaping and the construction stage analysis of cable-stayed bridges having moderate span lengths.

6. Bending moments in the main girder can be always localized by applying the G.TCUD method but the maximum moments in pylons in case of the unbalanced cable-stayed bridge can be extremely huge than those in the *balanced* bridge which means that the weight balancing between the center span and side spans should be carefully taken into account in the preliminary design.

7. Finally, it is judged that ULM3 and ULM4 based on the unstrained-lengths by AM3 and G.TCUD, respectively, can be the most powerful tool for not only the initial shaping analysis but also the subsequent construction stage analysis and structural nonlinear analysis under various load combinations.

REFERENCES

[1] Wang PH, Tseng TC, Yang CG. "Initial shape of cable-stayed bridges,"Comput Struct 1993;46(6): pp. 1095-1106.

[2] Chen DW, Au FTK, Tham LG, Lee PKK, "Determination of initial cable forces in prestressed concrete cable-stayed bridges for given design deck profiles using the force equilibrium method," Comput Struct 2000;74:pp. 1-9.

[3] Takagi R, Nakamura T, Nakagawa K. "A new design technique for pre-stressed loads of a cable-stayed bridge,"Comput Struct1995;58:pp. 607-612.

[4] Negrao JHP, Simoes LMC. "Optimization of cable-stayed bridges with three dimensional modeling,"Comput Struct1997;64:pp. 741-748.

[5] M. M. Hasan, A. O. Nassef, A. A. El Damatty (2012), "Determination of optimum post-tensioning cable forces of cable-stayed bridges,"Eng StructVol.44, pp. 248-259.

[6] Wang PH, Lin HT, Tang TY. "Study on nonlinear analysis of a highly redundant cable-stayed bridge," Comput Struct 2002;80:pp. 165-182.

[7] Kim KS, Lee HS."Analysis of target configurations under dead loads for cable-supported bridges,"Comput Struct 2001;79:pp. 2681-2692.

[8] Kim HK, Kim MY. "Efficient combination of aTCUDmethod and an initial force method for determining initial shapes of cable-supported bridges,"Int J of Steel Structures 2012;12(2):pp. 157-174.

[9] Kim MY, Kim DY, Jung MR, Attard MM. "Improved methods for determining the 3 dimensional initial shapes of cable-supported bridges," Int J of Steel Structures 2014;14(1):pp. 83-102.

[10] Jung MR, Min DJ, Kim MY. "Nonlinear analysis methods based on the unstrained element length for determining initial shaping of suspension bridges under dead loads, "Comput Struct 2013;128:pp. 272-285.

[11] Jayaraman, HB., Knudson, WC. "A curved element for the analysis of cable structures," Comput. Struct. 1981;14(3-4):pp. 325-333.

[12] Irvine, HM. "Cable structures,"1981.

[13] PacosteC, Eriksson A. "Beam elements in instability problems,"Comput Methods Appl Mech Engrg, 1997; 144:pp. 163-197.

[14] Crisfield,MA. "Non-linear finite element analysis of solids and structures," vol 1. Wiley, Chischester, 1997; pp. 201-233.

[15] LeTN, Battini JM. "Efficient formulation for dynamics of co-rotational 2D beams," Comput Mech 2011;48:pp. 153-161.

[16] Lozano-Galant JA, Dong XU, Paya-Zaforteza I, Turmo J. "Direct simulation of the tensioning process of cable-stayed bridges, "Comput Struct 2013;121:pp. 64-75.

APPENDIX

The followings are detailed forms of elastic stiffness, stiffness due to member deformations, geometric stiffness due to member forces and the unstrained length-related stiffness consisting of the extended tangential stiffness matrix of a frame element:

$$\mathbf{k}_{\mathbf{fu}}^{*} = \frac{EAD_1}{L_o^2}\begin{bmatrix} 1 \\ \frac{D_2+D_3}{-30} \\ \frac{4D_2-D_3}{-30} \\ -1 \\ \frac{D_2+D_3}{30} \\ \frac{D_2-4D_3}{30} \end{bmatrix}$$

$$\mathbf{k}_{\mathbf{e}}^{*}=\frac{EI}{L^{3}}\begin{bmatrix} AL^{2}/I & \cdot & \cdot & -AL^{2}/I & \cdot & \cdot \\ & 12 & 6L & \cdot & -12 & 6L \\ & & 4L^{2} & \cdot & -6L & 2L^{2} \\ & & & AL^{2}/I & \cdot & \cdot \\ & & & & 12 & -6L \\ \textit{symm.} & & & & & 4L^{2} \end{bmatrix}$$

$$\mathbf{k}_{\mathbf{d}}^{*}=\frac{EA}{30}\begin{bmatrix} \cdot & \frac{3(D_2+D_3)}{-L} & -4D_2+D_3 & \cdot & \frac{3(D_2+D_3)}{L} & D_2-4D_3 \\ & \frac{3(D_2+D_3)^2}{10L} & \frac{(4D_2-D_3)(D_2+D_3)}{10} & \frac{3(D_2+D_3)}{L} & \frac{3(D_2+D_3)^2}{-10L} & \frac{(-D_2+4D_3)(D_2+D_3)}{10} \\ & & \frac{(4D_2-D_3)^2L}{30} & 4D_2-D_3 & \frac{(4D_2-D_3)(D_2+D_3)}{-10} & \frac{L_o(4D_2^{\,2}-17D_2D_3+4D_3^{\,2})}{-30} \\ & & & \cdot & \frac{3(D_2+D_3)}{-L} & -D_2+4D_3 \\ & \textit{sym.} & & & \frac{3(D_2+D_3)^2}{10L} & \frac{(-D_2+4D_3)(D_2+D_3)}{-10} \\ & & & & & \frac{(D_2-4D_3)^2L}{30} \end{bmatrix}$$

$$\mathbf{k}_{\mathbf{g}}^{*}=\frac{P_1}{L}\begin{bmatrix} \cdot & \cdot & \cdot & \cdot & \cdot & \cdot \\ & 6/5 & L/10 & \cdot & -6/5 & L/10 \\ & & 2L^{2}/15 & \cdot & -L/10 & -L^{2}/30 \\ & & & \cdot & \cdot & \cdot \\ & \textit{sym.} & & & 6/5 & -L/10 \\ & & & & & 2L^{2}/15 \end{bmatrix}+\frac{P_2+P_3}{L}\begin{bmatrix} \cdot & 1 & \cdot & \cdot & -1 & \cdot \\ & \cdot & \cdot & -1 & \cdot & \cdot \\ & & \cdot & \cdot & \cdot & \cdot \\ & & & \cdot & \cdot & \cdot \\ & \textit{sym.} & & & 1 & \cdot \\ & & & & & \cdot \end{bmatrix}$$